

Optical Beam Splitter and Focuser in Ti:LiNbO₃ Planar Waveguide

L. Tsonev

Bulgarian Academy of Sciences, Institute of Solid State Physics, Boul. Lenin 72, BG-1184 Sofia, Bulgaria

Received 27 July 1983/Accepted 6 November 1983

Abstract. A *A*-type two-electrode system on a Ti diffused optical waveguide in LiNbO₃ has been studied in symmetrical and in asymmetrical operation regimes. In the first case the device acts as a beam splitter or focuser, depending on the polarity of the applied voltage. In the second case the device acts as a scanner. The driving voltage is relatively low. Possible applications are optical communication systems and optical processing of information.

PACS: 42.80.Ks, 42.80.Sa, 42.82.+n

At present a variety of optical thin-film guided-wave scanning deflectors and beam splitters exists, such as electro-optical prism [1], Bragg-deflector [2], TIR deflector [3, 4].

One of the most simple designs is the *A*-type two-electrode system, proposed in [1], for the operation in an asymmetrical regime – the light beam propagates in the waveguide parallel to one of the electrodes. According to the authors' intention this device must work as a scanner. In practice, this design has not been tested and examined. Up to now the investigations were directed toward another configuration, proposed in the same article [1] – the *N*-type three-electrode system with the light beam propagating parallel to the side electrodes [1, 5, 6]. In practice, several *N*-type systems are used together, forming an electrooptic phase diffraction grating. The grating deflects the light beam into a few discrete positions, when an appropriate electric field is applied.

In the present work a new operating regime for the *A*-type two-electrode system is proposed – a symmetrical regime, assuming that the light beam propagates along the bisectrix of the electrodes. This regime allows splitting and scanning or focusing of the light beam depending on the polarity of the applied voltage. The device described here can find applications in integrated optics, fiber transmission systems or signal processing systems. It has the potential for large

information handling capacity, high speed and low electrical drive power.

1. Theoretical Consideration

It is useful and very convenient to illustrate the device operation from a geometrical optics point of view. Two metal strip electrodes are deposited at an angle 2ψ onto a Ti-diffused planar optical waveguide in LiNbO₃ (Y-cut). The bisectrix of 2ψ is parallel to the *X*-axis of the crystal. The guided laser beam with TE polarisation propagates along the *X*-axis, too (Fig. 1a). Therefore we consider only TE modes and extraordinary indices of refraction N_e .

When a voltage is applied to the electrodes the effective mode index in the guide region between the electrodes is changed from N_m^* to $N_m^* \pm \Delta N_m^*$. Crossing the boundaries of the interelectrode area, each of the half-beams will be refracted. At a voltage, which reduces the effective index between the electrodes, the two half-beams are deflected to opposite directions, i.e. one can expect splitting of the input optical power into two output beams, the angle ϱ between them depending on the absolute voltage value (Fig. 1b). The voltage, which increases the effective index between the electrodes, causes crossing and overlapping of the two half-beams – the output beam becomes narrower than the input

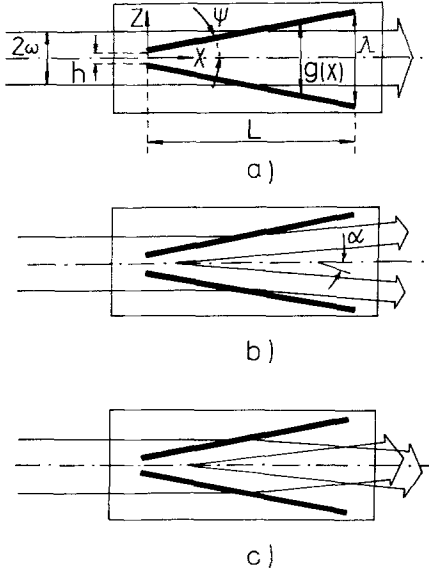


Fig. 1a-c. Top view scheme of the A -type electrode system on a planar waveguide in a symmetrical regime of operation (a) without applied voltage, (b) with applied positive voltage, (c) with applied negative voltage

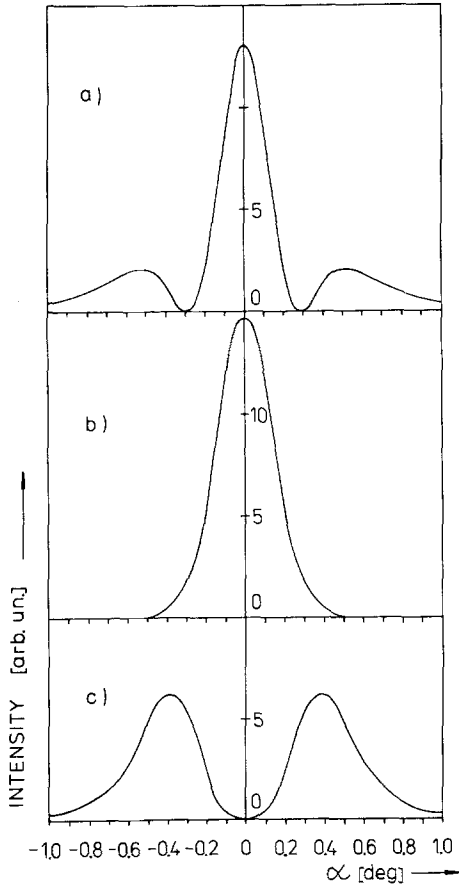


Fig. 2a-c. Far-field light intensity distribution according to (1) and (5) for: (a) $U = -12.5$ V, (b) $U = 0$ V, (c) $U = 12.5$ V. The function $I(\alpha)$ is normalized in such a way that the value of the integral $\int I(\alpha) d\alpha$ remains constant for different voltages

one. Due to this focusing effect one can expect to observe even an interference pattern in the far-field intensity distribution (Fig. 1c). Of course, the effects are symmetrical referring the bisectrix of the electrode system.

It is also possible to consider the behaviour of the present splitter-focuser by wave-optics methods. We used the following formula for the angular far-field distribution of the light intensity $I(\alpha)$ [5]:

$$I(\alpha) \sim \left\{ \int_{-A/2}^{A/2} \exp[-(z/\omega)^2] \cdot \cos[\varphi(z) - k\alpha z] dz \right\}^2, \quad (1)$$

where A is the maximum distance between the electrodes, 2ω is the minimum $1/e^2$ -width of the Gaussian guided beam, $k = 2\pi/\lambda_0$, λ_0 is the wavelength, α is a deviation angle, measured from the bisectrix, and $\varphi(z)$ is the phase change, accumulated over the device length L :

$$\varphi(z) = k \int_0^L N_m^*(U, x, z) dx. \quad (2)$$

When a voltage U is applied to the electrodes the guide effective index N_m^* becomes equal to

$$\begin{aligned} N_m^*(U, x, z) &= N_m^* \pm \Delta N_m^*(U, x, z) \\ \Delta N_m^*(U, x, z) &= \Delta N_m^*(U) f(z)/g(x), \\ \Delta N_m^*(U) &= (1/2)(N_m^*)^3 r_{33} (2/\pi) U \end{aligned} \quad (3)$$

due to the linear electrooptic effect.

Here $g(x)$ is the interelectrode distance, measured at a given x , $f(z)$ is a function, describing the transverse distribution of the effective index of refraction. We approximate the actual distribution $f(z)$ as follows

$$f(z) = \begin{cases} 0 & \text{for } |z| > (h/2) + x \tan \psi \\ 1 & \text{for } |z| < (h/2) + x \tan \psi, \end{cases} \quad (4)$$

where h is the spacing between inner electrode edges. Then the evaluation of $\varphi(z)$ from (2-4) leads to the expression

$$\varphi(z) = \begin{cases} kN_m^*L + k \frac{\Delta N_m^*(U)}{2 \tan \psi} \ln \frac{A/2}{|z|} & \text{for } |z| > h/2 \\ kN_m^*L + k \frac{\Delta N_m^*(U)}{2 \tan \psi} \ln \frac{A/2}{h/2} & \text{for } |z| < h/2. \end{cases} \quad (5)$$

Substituting (5) into (1) and carrying out the numerical calculations, we have obtained the far-field intensity distribution $I(\alpha)$, presented in Fig. 2.

2. Experimental Investigations

We used a planar waveguide formed by Ti diffusion in Y-cut LiNbO_3 . The guide supports two TE modes along the X -axis and their effective indices are $N_0^* = 2.2036$, $N_1^* = 2.2012$. The index of the bulk ma-

material is $N_{\text{bulk}} = 2.2000$. Assuming a Gaussian refractive index profile, we have found the surface index $N_{\text{surf}} = 2.2074$ and the effective layer thickness $y_{1/e} = 5.6 \mu\text{m}$. The attenuation is below 1 dB/cm for both modes with $m=0$ and 1.

The electrode system has the following characteristics: thickness of the Al layer $0.1 \mu\text{m}$, strip width $10 \mu\text{m}$, minimum interelectrode distance $h = 10 \mu\text{m}$, maximum interelectrode distance $A = 160 \mu\text{m}$, electrode length (measured along the bisectrix) $L = 10 \text{mm}$, angle between the electrode strips $2\psi = 0.8^\circ$, capacitance (measured at low frequencies) 3 pF. There is not any buffer layer under the electrodes. This fact does not cause any additional attenuation, but leads to beam broadening – larger for the $m=0$ mode than for the $m=1$ mode. Therefore all the experiments are carried out with the $m=1$ mode.

The laser beam has a Gaussian shape, with divergence of $2 \cdot 10^{-2}$ and with minimum $1/e^2$ -diameter $2\omega = 80 \mu\text{m}$. The input- and output-coupling are realized by SrTiO₃ prisms.

The electrodes are connected to the both poles of a controllable dc voltage source. The light coupled out from the device is recorded by a TV camera and displayed on a TV monitor. First, the beam is directed along the bisectrix of the electrode system visually – by a microscope. After this the beam position is chosen more precisely following the device behaviour when a dc voltage is applied (the sample holder has x -, z -translations and a y -rotation).

When one applies a voltage of such a polarity, which causes a refractive index decrease in the interelectrode area, the guided beam is splitted into two half-beams with equal intensities – in this case we shall speak about a positive voltage ($U > 0$). With increasing $|U|$ the beams scan in opposite directions; the maximum effect is achieved at $U = 10 \text{V}$ (Fig. 3d–g). The angular separation ϱ between the output halfbeams is presented at the right-hand side of Fig. 4 as a function of $U > 0$.

When a voltage of opposite polarity is applied, which increases the index of refraction in the interelectrode area, the guided beam becomes narrower – in this case we shall speak about a negative voltage ($U < 0$). With increasing $|U|$ the focusing effect becomes stronger and stronger, but for $U \leq -10 \text{V}$ the output beam is no longer a Gaussian one (Fig. 3d, c, b). The overlapping of the two half-beams causes the appearance of interference minima and maxima in the intensity distribution $I(\alpha)$ (Fig. 3a). The beam divergence σ is presented at the left-hand side of Fig. 4 as a function of $U < 0$.

At voltages $|U| > 10 \text{V}$ the output intensity distribution is rather complicated and inconvenient for practical use.

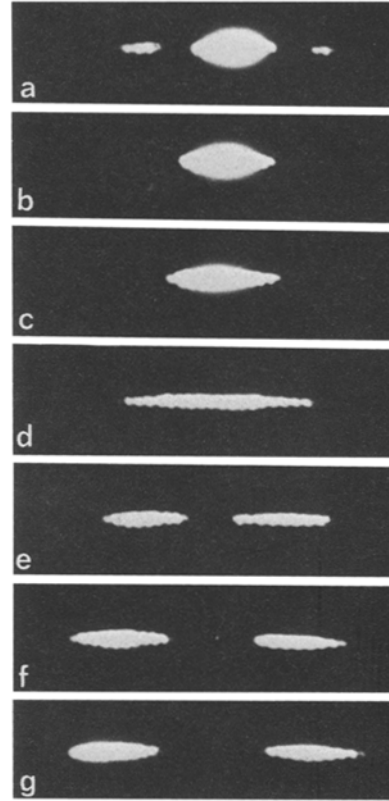


Fig. 3a–g. Photographs of the actual far-field light intensity distribution for $U =$: (a) -10V , (b) -7V , (c) -3.5V , (d) 0V , (e) 3.5V , (f) 7V , (g) 10V

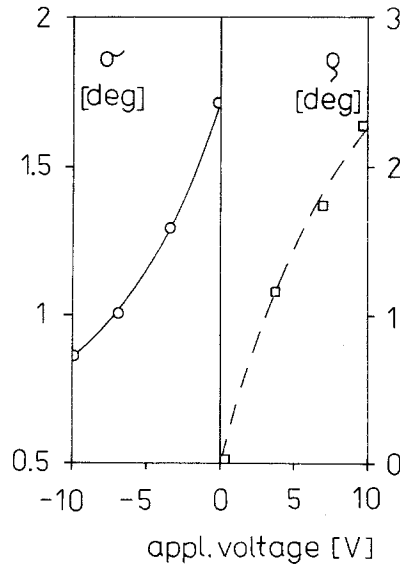


Fig. 4. Experimental values of the angular separation ϱ of both output half-beams for $U > 0$ and angular divergence σ of output beam for $U < 0$ vs. dc voltage. ϱ is the angle between the directions of maximum intensity, and σ is the angle between directions whose intensity is $1/e^2$ of the maximum one

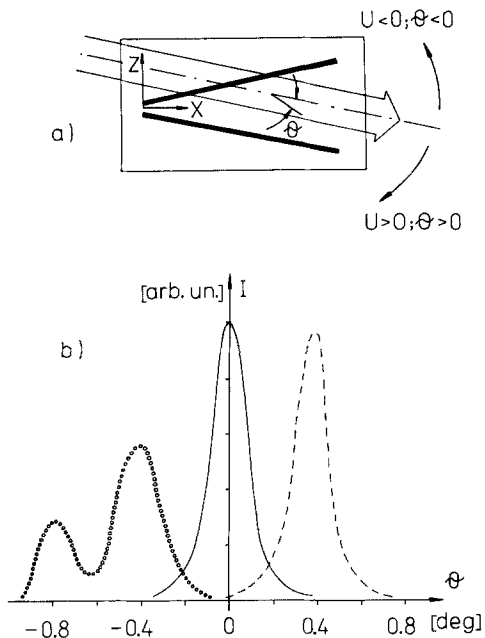


Fig. 5a and b. *A*-type electrode system in an asymmetrical operation regime. (a) Top view scheme. (b) Experimental output light intensity distribution for different voltages (— $U=0$ V, --- $U=18$ V, $\circ \circ \circ U=-18$ V)

In result we have:

- 1) A voltage of 3 V is enough for beam splitting at a $1/e^2$ -level (Fig. 3e).
- 2) At 7 V the angular separation between the output halfbeams is equal to the angular divergence of each halfbeam (Fig. 3f).
- 3) At -7 V the output beam divergence is two times smaller than at 0 V, without disturbing the Gaussian intensity distribution (Fig. 3b).
- 4) A good qualitative and even quantitative agreement between the wave optics model (Fig. 2) and the experiment (Fig. 3a and g) is observed.

A possible application of the device, described here, is the commutation of an optical signal between a central fibre and two neighbour side fibres.

The sample is also studied in the asymmetrical regime, when the guided beam (with a divergence of 10^{-4})

propagates parallel to one of the electrodes (Fig. 5a). Applying dc voltage, we observe a simple beam scanning – to the parallel electrode or to the slanted one – according to the direction of the electric field. The intensity distribution as a function of the applied voltage is presented in Fig. 5b. When the beam is deflected to the slanted electrode, its structure changes – the beam becomes wider and even splits because of its partial penetration under this electrode ($U = -18$ V). When the beam is deflected to the parallel electrode, there are not such structural disturbances, at least up to $U = 18$ V. As it was already mentioned, this operation regime of the *A*-electrode structure has been suggested in [1], but up to now there are not published data about its experimental realization.

3. Conclusions

An already known electrode structure on a planar electrooptic waveguide is investigated in a new regime, which allows to find two new functional possibilities of this structure for the purposes of integrated optics, fibre optics and signal processing – splitting and focusing of the guided laser beam. Both effects are obtained at low drive voltages ($|U| < 10$ V). The operating principle is looked at from the geometrical-optics and from the wave-optics point of view.

The device is also tested in a scanner regime, as it was primarily suggested in [1]. A satisfactory beam scanning is observed at voltages between 10 and 20 V.

Acknowledgements. The author thanks Dr. I. Savatinova for the critical reading of the manuscript.

References

1. C.S. Tsai, P. Saunier: Appl. Phys. Lett. **27**, 248–250 (1975)
2. J.M. Hammer, W. Phillips: Appl. Phys. Lett. **24**, 545–547 (1974)
3. S.K. Sheem: Appl. Opt. **17**, 3679–3687 (1978)
4. I. Savatinova, S. Tonchev: Appl. Phys. A **31**, 187–190 (1983)
5. S.I. Bozhevol'nyi, E.M. Zolotov, A.M. Prokhorov, V.A. Chernykh, E.A. Shcherbakov: Kvantovaya Elektron. **7**, 1778–1783 (1980) (in Russian)
6. C.H. Bulmer, W.K. Burns, T.G. Giallorenzi: Appl. Opt. **18**, 3282–3295 (1979)